Chemical Diffusion in the Iridium-Rich A1 and L12 Phases in the Ir-Nb System

AUTHOR(S):

Numakura, Hiroshi; Watanabe, Tatsuru; Uchida, Makoto; Yamabe-Mitarai, Yoko; Bannai, Eisuke

CITATION:

Numakura, Hiroshi ...[et al]. Chemical Diffusion in the Iridium-Rich A1 and L12 Phases in the Ir-Nb System. Journal of phase equilibria and diffusion 2006, 27(6): 638-643

ISSUE DATE:

2006

URL:

http://hdl.handle.net/2433/48904

JPEDAV (2006) 27:638-643
DOI: 10.1361/154770306X153666
1547-7037/$19.00 ©ASM International

Chemical Diffusion in the Iridium-Rich *A*1 and $L1_2$ Phases in the Ir-Nb System

Hiroshi Numakura, Tatsuru Watanabe, Makoto Uchida, Yoko Yamabe-Mitarai, and Eisuke Bannai

(Submitted April 4, 2006; in revised form June 15, 2006)

The diffusion in iridium-rich Ir-Nb alloys has been studied by single-phase interdiffusion experiments. The chemical diffusion coefficient has been measured for the primary fcc solid-solution and the $L1_2$ ordered compound Ir_3Nb in the temperature range between 1650 and 1950 °C, using Ir/Ir-8Nb and Ir-26Nb/Ir-28Nb diffusion couples, respectively (numbers indicate mol%). While the chemical diffusion coefficient in the solid-solution phase is close to the tracer self-diffusion coefficient of pure iridium, the diffusion in the compound phase is extremely slow: the chemical diffusion coefficient is ¼₀ to ⅕₀ of that in the solid solution. The low diffusion rate in the compound must be beneficial for high-temperature performance of refractory superalloys based on the Ir-Nb system.

Keywords binary interdiffusion, chemical diffusion, intermetallic compound, iridium-niobium alloys, solid-solution

1. Introduction

Alloys based on iridium, rhodium, and platinum are attracting growing interest recently as ultrahigh-temperature materials: the expected operating temperatures far exceed those of the current nickel-base superalloys.[1] While the microstructure, mechanical properties, and their relationships have been studied extensively,[2,3] much work is still needed on the basic, that is, thermodynamic and kinetic, properties, in particular atomic diffusion, which controls the stability and performance of materials at elevated temperatures.

A leading candidate for refractory superalloys of the next generation is the two-phase ($A1$ + $L1_2$) Ir-Nb alloys,[2,3] which is an analog of the nickel-base $\gamma + \gamma'$ superalloys. In the present investigation, the authors have studied the diffusion in the constituent phases: the chemical diffusion coefficient in the $A1$ [face-centered cubic (fcc) solid-solution] and in the $L1_2$ ordered compound have been measured by single-phase interdiffusion experiments, aiming at providing basic information on the kinetic properties required for material design of the two-phase alloys. Part of the present work concerning the $L1_2$ phase was reported earlier.[4] This paper presents the whole set of data, including the latest experimental results on the $A1$ solid-solution phase.

This article was presented at the Multicomponent-Multiphase Diffusion Symposium in Honor of Mysore A. Dayananda, which was held during TMS 2006, 135th Annual Meeting and Exhibition, March 12-16, 2006, in San Antonio, TX. The symposium was organized by Yongho Sohn of University of Central Florida, Carelyn E. Campbell of National Institute of Standards and Technology, Richard D. Sisson, Jr., of Worcester Polytechnic Institute, and John E. Morral of Ohio State University.

Hiroshi Numakura, Tatsuru Watanabe, and **Makoto Uchida,** Department of Materials Science and Engineering, Kyoto University, Sakyo-ku, Kyoto 606–8501, Japan; **Yoko Yamabe-Mitarai** and **Eisuke Bannai,** National Institute for Materials Science, Sengen 1-2-1, Tsukuba 305-0047, Japan. Contact e-mail: hiroshi-numakura@mtl.kyoto-u.ac.jp.

2. Experimental

2.1 Specimens

Coarse-grained polycrystals (grain size > 0.1 mm) and single crystals of pure iridium, Ir-8Nb, Ir-26Nb, and Ir-28Nb alloys were used, where the numbers denote the concentration of Nb in mol%. The sample rods, about 5 mm in diameter and 20 mm in length, were grown by optical floating-zone melting. The exact compositions of the alloys were determined by electron probe microanalysis.

Disks of about 3 mm in thickness were sectioned by a spark-erosion wire saw. After polishing the surfaces, each pair of disks, either of Ir/Ir-8Nb or of Ir-26Nb/Ir-28Nb, was diffusion-bonded by annealing at 1400 or 1500 °C for 1 h in a vacuum under a uniaxial compressive stress of 10 MPa. Each pair was then cut perpendicularly to the bonded interface into four pieces. The diffusion couples thus prepared were diffusion annealed in a vacuum maintained below 5×10^{-4} Pa.

2.2 Measurements of Concentration Profiles

Composition versus distance profiles were measured using a wavelength-dispersive electron probe microanalyzer, with an acceleration voltage of 15 kV, a beam current of 10 nA and a probe size of about 1 μm. The intensities of Ir Mα and Nb Lα characteristic x-rays were measured by step-scanning across the bonded interface over a distance of about five to ten times the expected diffusion distance. The composition at each point was calculated from the intensities with the standard ZAF correction[5] using polished pieces of pure iridium and pure niobium as reference materials. Three profiles were obtained and were averaged to reduce statistical errors.

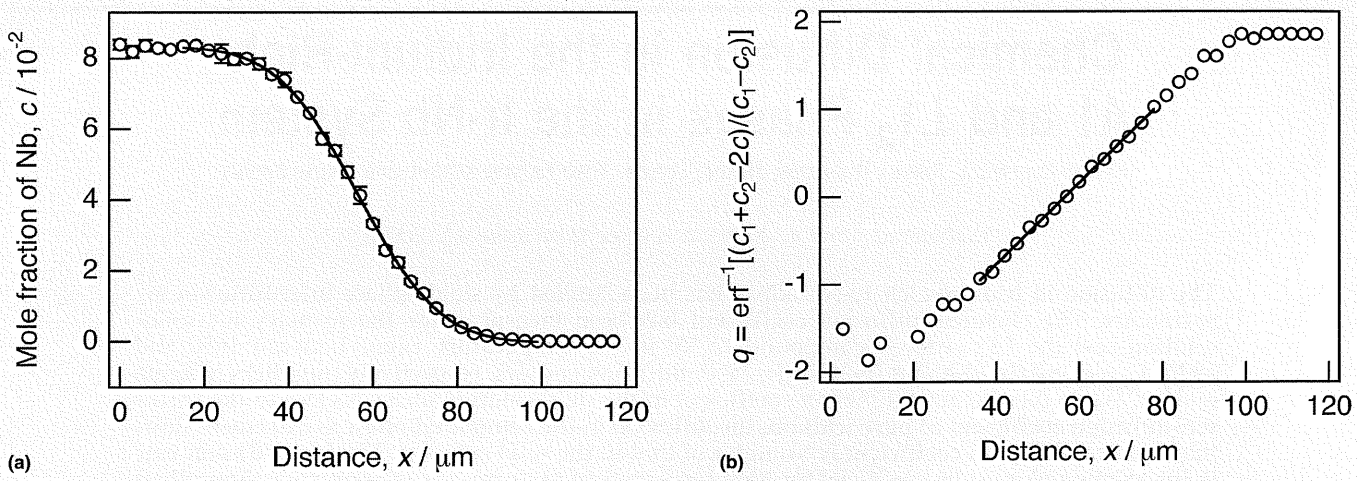

Fig. 1 (a) The concentration profile in an Ir/Ir-8Nb diffusion couple annealed at 1750 °C for 168 h and (b) its probability plot. The solid curve in (a) is the error function profile fitted to the measured points (circles), and the solid line in (b) is the result of linear regression.

3. Results and Discussion

3.1 Determination of the Diffusion Coefficient

Figure 1(a) shows the averaged concentration profile in an Ir/Ir-8Nb diffusion couple annealed at 1750 °C for 168 h, given in terms of the mole fraction of Nb. The solid line is the standard error-function profile:

$$c(x,t) = \frac{c_1 + c_2}{2} - \frac{c_1 - c_2}{2} \operatorname{erf}\left(\frac{x - x_0}{2\sqrt{Dt}}\right) \qquad \text{(Eq 1)}$$

which has been fitted to the measured data points. In the fitting, c_1 and c_2 (the terminal concentrations), x_0 (the coordinate center), and $2\sqrt{Dt}$ (the diffusion distance, with t the annealing time) have been adjusted. From the diffusion distance evaluated by the fitting, the diffusion coefficient D (the chemical diffusion coefficient) is obtained. The fitting has been done for the data points encompassing about four times the diffusion distance, that is, 8 $\sqrt{Dt}$. In this particular example, the diffusion distance is found to be 21.55 ± 0.39 μm, from which D is calculated to be (1.92 ± 0.07) × 10^{16} m^2s^{-1}. Figure 1(b) presents a "probability plot" of the concentration profile; the measured values of $c = c(x, t)$ has been converted by the inverse error function to:

$$q(x,t) = \operatorname{erf}^{-1}\left(\frac{c_1 + c_2 - 2c}{c_1 - c_2}\right) \qquad \text{(Eq 2)}$$

using the values of c_1 and c_2 determined by the fitting of the error-function profile. If the concentration profile follows the standard form of Eq 1, this plot is to appear as a straight line, which is actually the case for Fig. 1(b). The slope of the plot, which equals $1/(2\sqrt{Dt})$, has been evaluated by linear regression to the data points in the region where $-1 < q < +1$, which corresponds to about twice the diffusion distance. The diffusion distance, $2\sqrt{Dt}$, thus evaluated for Fig. 1(b) is 21.51 ± 0.25 μm, giving the diffusion coefficient D = (1.91 ± 0.04) × 10^{-16} m^2s^{-1}. The probability plot was linear not only for this example, but also for the profiles of all the other Ir/Ir-8Nb diffusion couples annealed at different temperatures, and consequently the values of the diffusion coefficient determined by the two methods agree well with each other. The linear probability plots indicate that the chemical diffusion coefficient in the solid-solution phase is virtually independent of composition in the range from 0 to 8% Nb, in the temperature range from 1650 to 1900 °C.

An example of the results for Ir-26Nb/Ir-28Nb diffusion couples is shown in Fig. 2, where the concentration profile (a) and its probability plot (b) for the couple annealed at 1850 °C for 288 h are presented. The diffusion turned out much slower than expected, and not as many number of points could be measured in the diffusion zone as for the solid-solution couples; the minimum step width was limited to 2 μm by the probe size, which was about 1 μm. If the diffusion coefficient varies with composition, which is very likely in intermetallic compounds even for a narrow range of composition,[6] the concentration profile would deviate from the error function profile, and correspondingly its probability plot would be curved. However, it is difficult to distinguish if the probability plot is curved or not for the present data because of the limited number of points and the relatively large scatter; the latter is due to the small composition difference between the two members of the couple. The probability plot for the 26Nb/28Nb was thus analyzed by linear regression, assuming tentatively a constant diffusion coefficient. The chemical diffusion coefficient evaluated for the $L1_2$ diffusion couples, which were annealed at 1750 to 1950 °C, by the two methods are listed in the lower part of Table 1. The error margins are much larger than those for the solid-solution couples, but the mean values of D from the two methods fall within each other's margins. In both the $A1$ and $L1_2$ diffusion couples, the difference in the molar volume between the two members of the couple is about 0.25%, which is small and thus was not taken into account in the analyses.

3.2 Temperature Dependence of Diffusion

Figure 3 shows Arrhenius plots of the chemical diffusion coefficients in the $A1$ and $L1_2$ phases. The values obtained

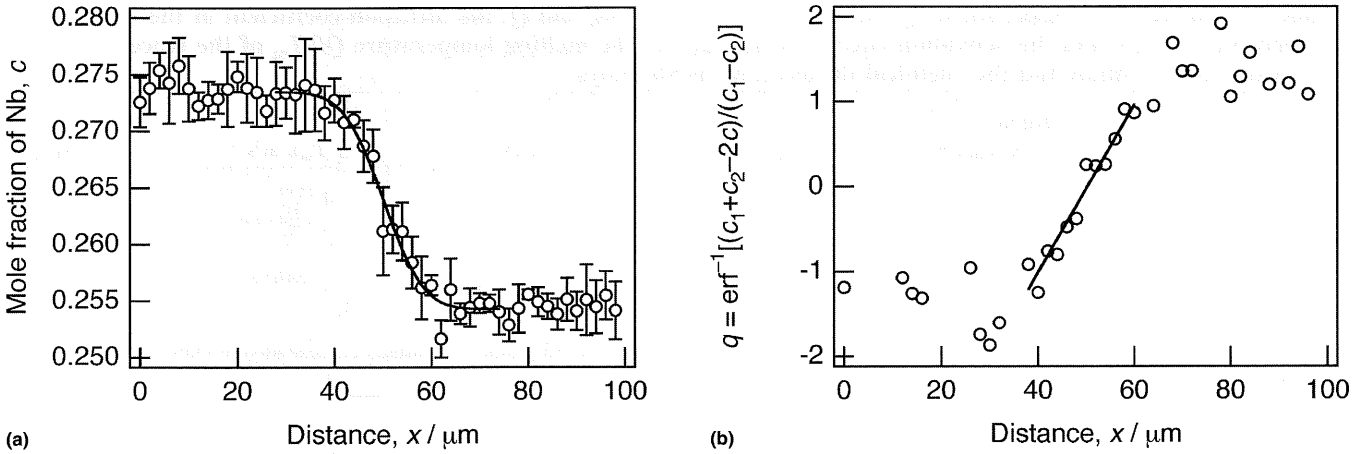

Fig. 2 (a) The concentration profile in an Ir-26Nb/Ir-28Nb diffusion couple annealed at 1850 °C for 288 h and (b) its probability plot. The mode of presentation is the same as in Fig. 1.

Table 1 Diffusion distance $2\sqrt{Dt}$ and chemical diffusion coefficient D in the $A1$ (solid-solution) and $L1_2$ (ordered compound) phases of Ir-Nb alloys obtained from Ir/Ir-8Nb (0/8) and Ir-26Nb/Ir-28Nb (26/28) diffusion couples annealed at temperature T for time t

Temperature (T), °C	Time (t), h	$2\sqrt{Dt}$, μm	D, m^2s^{-1}
0/8			
1650	672	20.44 ± 0.45	(4.32 ± 0.19) × 10^{-17}
		20.09 ± 0.45	(4.17 ± 0.19) × 10^{-17}
1700	312	19.54 ± 0.54	(8.50 ± 0.47) × 10^{-17}
		20.12 ± 0.35	(9.01 ± 0.31) × 10^{-17}
1750	168	21.55 ± 0.39	(1.92 ± 0.07) × 10^{-16}
		21.51 ± 0.25	(1.91 ± 0.04) × 10^{-16}
1850	96	32.29 ± 0.79	(7.54 ± 0.37) × 10^{-16}
		32.06 ± 0.51	(7.44 ± 0.24) × 10^{-16}
1900	64	37.17 ± 0.75	(1.50 ± 0.06) × 10^{-15}
		37.45 ± 0.43	(1.52 ± 0.03) × 10^{-15}
26/28			
1750	1128	8.21 ± 1.11	(4.15 ± 1.12) × 10^{-18}
		7.61 ± 0.63	(3.57 ± 0.59) × 10^{-18}
1800	384	6.19 ± 1.34	(0.69 ± 0.30) × 10^{-17}
		7.47 ± 1.22	(1.01 ± 0.33) × 10^{-17}
1850	288	9.13 ± 1.17	(2.01 ± 0.52) × 10^{-17}
		10.14 ± 0.78	(2.48 ± 0.38) × 10^{-17}
1900	192	9.01 ± 1.57	(2.94 ± 1.02) × 10^{-17}
		9.45 ± 1.11	(3.23 ± 0.76) × 10^{-17}
1950	96	8.14 ± 1.16	(4.79 ± 1.37) × 10^{-17}
		8.94 ± 0.94	(5.78 ± 1.22) × 10^{-17}

The two values of $2\sqrt{Dt}$ and D are those obtained by fitting the error function profile (first line) and by linear regression to the probability plot (second line), respectively.

from the probability plot have been adopted here, as those evaluated from the fitting of the error function profile were sensitive to the choice of the range of data used for the

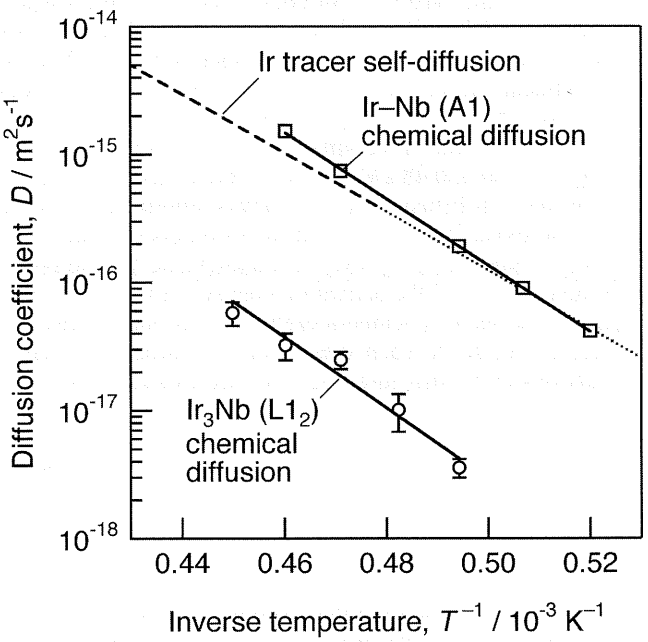

Fig. 3 Arrhenius plots of the chemical diffusion coefficients of Ir-Nb alloys of the $A1$ solid-solution phase and of the $L1_2$ compound phase evaluated by linear regression to the probability plot of the interdiffusion profile. The dashed line shows the tracer self-diffusion coefficient of pure iridium,[7] and the dotted line is its extension.

nonlinear fitting, and thus their accuracies were difficult to assess. In the same figure, the tracer self-diffusion coefficient of pure iridium as reported in the literature[7] is reproduced. The diffusion coefficients are found to obey the Arrhenius law and can be expressed as:

$$D = D_0 \exp\left(-\frac{Q}{kT}\right) \qquad \text{(Eq 3)}$$

where k is the Boltzmann constant and T is temperature. The values of the preexponential factor D_0 and the activation

Table 2 The melting temperature T_m, Arrhenuis parameters D_0 and Q, the diffusion coefficient at the melting temperature $D(T_m)$, and the activation energy normalized to the melting temperature Q/kT_m of the tracer self-diffusion of iridium and the chemical diffusion of Ir-Nb alloys

Phase	Melting temperature (T_m), K	D_0, m^2s^{-1}	Q, eV	$D(T_m)$, m^2s^{-1}	Q/kT_m
Ir, self ($A1$)	2720	$10^{-4.44}$	4.548	$10^{-12.87}$	19.40
Ir-Nb ($A1$)	2693(a)	$10^{-2.88\pm0.25}$	5.15 ± 0.10	$10^{-12.52\pm0.44}$	22.19 ± 0.43
		($10^{-2.91\pm0.42}$)	(5.14 ± 0.16)		
Ir_3Nb ($L1_2$)	2708	$10^{-3.7\pm1.1}$	5.49 ± 0.48	$10^{-13.9\pm2.0}$	23.5 ± 2.0
		($10^{-5.3\pm1.7}$)	(4.85 ± 0.71)		

The Arrhenius parameters in the parentheses are those obtained by fitting the error function profile to measured concentration profiles.
(a) The solidus temperature of Ir-4% Nb

energy Q have been determined by linear regression and are listed in Table 2, and those for the diffusion coefficients obtained by the error function fitting are also listed for reference. In the earlier, preliminary report on the diffusion in the $L1_2$ Ir_3Nb,[4] the authors evaluated the diffusion coefficient only in terms of the error-function profile, that is, by nonlinear fitting, and reported the activation parameters $D_0 = 10^{-5.3\pm1.1}$ m^2s^{-1} and $Q = 4.83 \pm 0.44$ eV. The present values based on the probability plots, $D_0 = 10^{-3.7\pm1.1}$ m^2s^{-1} and $Q = 5.49 \pm 0.48$ eV, are considered more reliable.

For the self-diffusion in pure metals, empirical rules are known to exist:[8] the tracer self-diffusion coefficient at the melting temperature T_m takes a similar value for metals of the same class, and the activation energy is roughly proportional to the melting temperature with a proportionality coefficient specific to each class. For the particular case of metals of the $A1$ structure, the rules are expressed as:

$$D(T_m) \approx 10^{-12.26}\ m^2s^{-1} \quad \text{(Eq 4a)}$$

$$Q \approx 18.4\ kT_m \quad \text{(Eq 4b)}$$

The diffusion properties of pure iridium and the Ir-Nb alloys are compared in the last two columns of Table 2 in reference to these relations. The self-diffusion behavior of pure iridium conforms well, in fact, to the empirical rule. The comparison for the chemical diffusion in the alloys is, however, tentative because chemical diffusion coefficients were never within the scope of the rules.[8] Moreover, particularly for intermetallic compounds, chemical diffusion may not even obey the Arrhenius law.[6] Nevertheless, this comparison may be useful to see the trends in diffusion in the materials of interest. The diffusivity in the Ir-Nb solid-solution alloys is similar in magnitude to pure fcc metals, but the activation energy is appreciably higher, leading to rapid decrease in the diffusion rate with decreasing temperature. The diffusion in the $L1_2$ compound Ir_3Nb is slower (as already evident in Fig. 3) at the melting temperature and slows down with decreasing temperature at a similar rate to the case of the solid-solution phase. From a practical viewpoint, the slow diffusion in the Ir-Nb alloys, particularly in the $L1_2$ phase, must be a good advantage for high-temperature applications: the alloys may show superior microstructural stability and resistance to diffusional creep deformation.

3.3 Chemical Diffusion and Tracer Diffusion

The chemical diffusion coefficient in a binary solid-solution alloy is related to the tracer diffusion coefficient of constituent species, D_1^* and D_2^*, by the formula derived by Darken[9] and later modified by Manning:[10]

$$D = (D_1^* c_2 + D_2^* c_1)\,\Phi S \quad \text{(Eq 5)}$$

where D_i^* and c_i are the tracer diffusion coefficient and the mole fraction of the constituent i, respectively, Φ is the thermodynamic factor, and S is the vacancy wind factor. Recent theoretical analyses suggest that, although not exactly but practically, this relation applies also to ordered alloys of the $L1_2$ structure, as well as some other ordered structures.[11,12]

On the basis of Eq 5, the chemical diffusion in the Ir-Nb solid-solution phase is governed primarily by the diffusion of Nb in the alloy because of the reciprocal arithmetic average. Since the thermodynamic factor approaches unity as either c_1 or c_2 goes to zero, the chemical diffusion coefficient at such extrema represents the tracer diffusion coefficient of the solute species, that is, the impurity diffusion coefficient. To evaluate the impurity diffusion coefficient from chemical diffusion data, it is usually necessary to carefully extrapolate the measured values of the chemical diffusion coefficient to the dilute limit. In the present case, however, such a procedure is not required since the chemical diffusion coefficient in the solid-solution phase is virtually independent of composition: the tracer diffusion coefficient of Nb in pure iridium is supposed to be equal to the chemical diffusion coefficient for the solid-solution phase obtained in this study, which is roughly equal to the tracer self-diffusion coefficient of iridium. There are no tracer diffusivity data for Nb reported in the literature with which to compare. The only data available with which to compare are the data on the tracer self-diffusion of niobium of the $A2$ [body-centered cubic (bcc)] structure,[7] which is not very relevant to the case in point.

According to an ongoing thermodynamic assessment of the Ir-Nb system,[13] the thermodynamic factor Φ in the

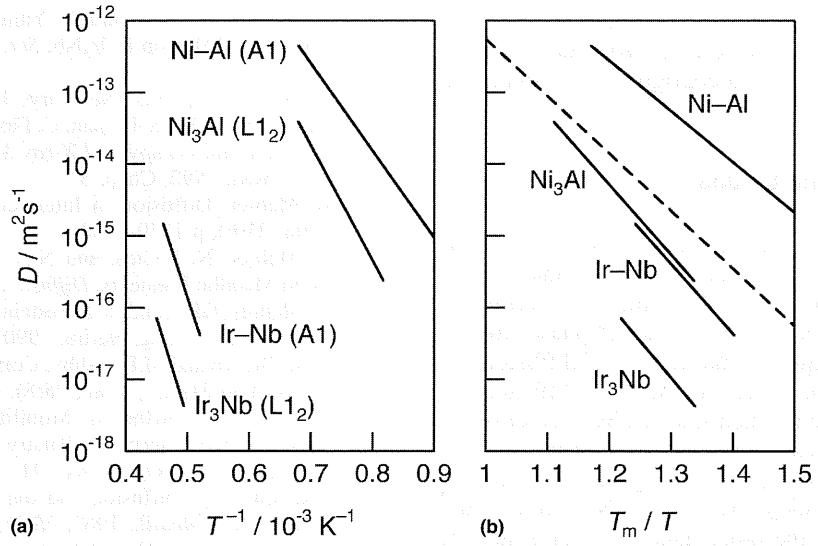

Fig. 4 (a) The chemical diffusion coefficients in the Ir-Nb solid-solution phase and in the Ir_3Nb phase (present work), and those in the Ni-Al solid solution phase[16] (at 4% Al) and in the Ni_3Al phase[12] (at 25% Al), as a function of inverse temperature and (b) of inverse homologous temperature. The dashed line in (b) is the empirical tracer self-diffusion coefficient in pure fcc metals.

solid-solution phase is estimated to be in the range from 1 to 2.5, gradually increasing with Nb content (from 1 at 0% Nb to 2.5 at 8% Nb), in the temperature range of the present diffusion data. Since the chemical diffusion coefficient remains unchanged in this range of composition, this estimation of Φ means that the tracer diffusion coefficients at 0 and 8% Nb are related as $D^*_{Nb}(0) \approx [0.08\ D^*_{Ir}\ (0.08) + 0.92 D^*_{Nb}\ (0.08)] \times 2.5$, where the numbers in parentheses indicate the mole fraction of Nb to which the diffusion coefficients refer. (The influence of the vacancy wind factor S is generally small and may be ignored except for detailed analyses.)[10-12] As the contribution of D^*_{Ir} is small, this relation indicates that D^*_{Nb} decreases with increasing Nb concentration to compensate for the enhancement of the chemical diffusion by the thermodynamic factor. How such lowering of the tracer diffusivity, if real, occurs is an intriguing problem, which should be clarified by more detailed studies. Short-range order, which must exist in the Ir-Nb solid-solution alloy, appears to be one of the possible origins; its effect on the atomic diffusion, possibly through the vacancy concentration, seems worth examining.

The effect of the thermodynamic factor is in general more pronounced in ordered alloys or intermetallic compounds: Φ can be much larger than in the solid-solution phase and may exhibit a sharp maximum at the stoichiometric composition in chemically stable compounds.[14,15] In the thermodynamic assessment,[13] the thermodynamic factor in Ir_3Nb is indeed predicted to be peaked at the stoichiometric composition, $c = 0.25$, where Φ reaches about 100. However, at hyperstoichiometric compositions ($c > 0.25$), Φ decreases sharply with Nb content, and in the composition range of the present experiment, 26 to 28% Nb, it continues to decrease but rather slowly, from 20 or 15. The influence of the small variation in Φ cannot be identified in the present experimental data, as a result of the large scatter. In any case, assuming that the Darken-Manning relation holds, the tracer diffusivities of Ir and Nb in Ir_3Nb are predicted to be even an order of magnitude lower than the already low chemical diffusivity.

3.4 Comparison with the Diffusion Behavior of Ni-Al Alloys

In the scope of developing novel high-temperature materials, comparing the diffusion behavior in the Ir-Nb alloys with that in the Ni-Al alloys is interesting, as was partly done for the $L1_2$ ordered phases, Ir_3Nb and Ni_3Al, in the previous paper.[4] Figure 4(a) shows the chemical diffusion coefficients in the $A1$ and $L1_2$ phases in the Ir-Nb system obtained in the present work and those in the Ni-Al solid-solution (γ) phase[16] (evaluated at 4% Al) and in the Ni_3Al (γ') phase[12] (evaluated at 25% Al). The diffusion coefficients of the Ir-Nb alloys have been measured at far higher temperatures, and extrapolating them to the range of temperature of the data for the Ni-Al alloys gives the diffusivities many orders of magnitude lower than those in the Ni-Al alloys.

A more convenient and possibly instructive comparison is made in Fig. 4(b), where the diffusion coefficients are plotted against the inverse homologous temperature, T_m/T. Here, the empirical formula for the tracer self-diffusion coefficients in pure fcc metals, $D = 10^{-12.26} \exp(-18.4\ T_m/T)\ m^2s^{-1}$, is also plotted, which may serve as a reference. The Arrhenius plots of the chemical diffusion coefficients in the Ni-Al solid-solution and Ni_3Al compound phases are located above and below this reference, respectively. On the other hand, the chemical diffusivity in the Ir-Nb solid-solution phase is already lower than the reference, and that in the Ir_3Nb compound finds itself farther below. With the same crystal structure as Ni_3Al and probably a similar mechanism of atom movements[17,18] operating at the corresponding homologous temperature range, how such striking difference in the diffusivities can occur is an intriguing

problem. To clarify its origin, it is necessary to study the thermodynamic properties and kinetic properties of point defects, that is, their equilibrium configurations, concentrations, and mobilities.

4. Summary and Conclusions

The chemical diffusion coefficients in Ir-Nb alloys of the $A1$ solid-solution and $L1_2$ ordered compound phases have been measured by single-phase interdiffusion experiments. The chemical diffusion coefficient in the $A1$ phase (from 0 to 8% Nb) is roughly equal to the tracer self-diffusion coefficient of pure iridium, while the chemical diffusion coefficient in the $L1_2$ phase is much smaller, by a factor of ¼0 to ⅕0. From a practical viewpoint, the slow diffusion in the compound phase is advantageous for high-temperature applications of two-phase alloys based on Ir-Nb. From a fundamental viewpoint, on the other hand, to understand the origins of the low diffusivities and to establish the scientific basis for material design, it is desirable to investigate the basic properties of point defects in these alloy phases in detail.

Acknowledgments

This work is partly supported by Grant-in-Aid for Scientific Research, Basic Research (C), 17560584, from the Ministry of Education, Culture, Sports, Science, and Technology, Japan.

References

1. Y. Yamabe-Mitarai, Y. Gu, C. Huang, R. Völkl, and H. Harada, Platinum-Group-Metal-Based Intermetallics as High-Temperature Structural Materials, *JOM,* 2004, **56**(9), p 34-39
2. Y. Yamabe-Mitarai, Y. Ro, T. Maruko, and H. Harada, Ir-Base Refractory Superalloys for Ultra-High Temperatures, *Metall. Mater. Trans. A,* 1998, **29A**(2), p 537-549
3. Y. Yamabe-Mitarai, Y. Gu, and H. Harada, Compressive Strength and Creep Properties of Ir-Nb-Zr Alloys between 1473 and 2073 K, *Metall. Mater. Trans. A,* 2003, **34A**(10), p 2207-2215
4. M. Uchida, H. Numakura, Y. Yamabe-Mitarai, and E. Bannai, Chemical Diffusion in Ir_3Nb, *Scr. Mater.,* 2005, **52**(1), p 11-15
5. J.I. Goldstein, D.E. Newbury, P. Echlin, D.C. Joy, A.D. Romig Jr., and C.E. Lyman, C. Fiori, and E. Lifshin, *Scanning Electron Microscopy and X-ray Microanalysis,* 2nd ed., Plenum Press, 1992, Chap. 8
6. H. Mehrer, Diffusion in Intermetallics, *Mater. Trans., JIM,* 1996, **37**(6), p 1259-1280
7. H. Mehrer, N. Stolica, and N.A. Stolwijk, Self-Diffusion in Solid Metallic Elements, *Diffusion in Solid Metals and Alloys,* H. Mehrer, Ed., Landolt-Börnstein New Series, Group III, Vol 26, Springer Verlag, Berlin, 1990, Chap. 2
8. A.M. Brown and M.F. Ashby, Correlations for Diffusion Constants, *Acta Metall.,* 1980, **28**(8), p 1085-1101
9. L.S. Darken, Diffusion, Mobility and Their Interrelation through Free Energy in Binary Metallic Systems, *Trans. AIME,* 1948, **175**(1), p 184-194
10. J.R. Manning, Diffusion and the Kirkendall Shift in Binary Alloys, *Acta Metall.,* 1967, **15**(5), p 817-826
11. I.A. Belova and G.E. Murch, Test of the Validity of the Darken/Manning Relation for Diffusion in Ordered Alloys Taking the $L1_2$ Structure, *Philos. Mag. A,* 1998, **78**(5), p 1085-1092
12. T. Ikeda, A. Almazouzi, H. Numakura, M. Koiwa, W. Sprengel, and H. Nakajima, Single-Phase Interdiffusion in Ni_3Al, *Acta Mater.,* 1998, **46**(15), p 5369-5376
13. T. Abe, Y. Chen, Y. Yamabe-Mitarai, and H. Numakura, in preparation
14. Y.A. Chang and J.P. Neumann, Thermodynamics and Defect Structure of Intermetallic Phases with the B2 (CsCl) Structure, *Prog. Solid State Chem.,* 1982, **14**(4), p 221-301
15. T. Ikeda, H. Numakura, and M. Koiwa, A Bragg-Williams Model for the Thermodynamic Activity and the Thermodynamic Factor in Diffusion for Ordered Alloys with Substitutional Defects, *Acta Mater.,* 1998, **46**(18), p 6605–6613; *idems,* corrigendum, *Acta Mater.,* 1999, **47**(6), p 1993
16. M. Watabane, Z. Horita, T. Sano, and M. Nemoto, Electron Microscopy Study of Ni/Ni_3Al Diffusion-Couple Interface—II. Diffusivity Measurement, *Acta Metall. Mater.,* 1994, **42**(10), p 3389-3396
17. H. Numakura, T. Ikeda, M. Koiwa, and A. Almazouzi, Self-Diffusion Mechanism in Ni-Based $L1_2$ Type Intermetallic Compounds, *Philos. Mag. A,* 1998, **77**(4), p 887-909
18. H. Numakura, T. Ikeda, H. Nakajima, and M. Koiwa, Diffusion in Ni_3Al, Ni_3Ga and Ni_3Ge, *Mater. Sci. Eng. A,* 2001, **312**(1-2), p 109-117